Liquid-Crystalline Octopus Dendrimers: Block Molecules with Unusual Mesophase Morphologies

Lionel Gehringer, Cyril Bourgogne, Daniel Guillon, and Bertrand Donnio*

Contribution from the Institut de Physique et Chimie des Matériaux de Strasbourg – IPCMS, Groupe des Matériaux Organiques – GMO, UMR 7504 – CNRS/Université Louis Pasteur, 23, rue du Loess, BP 43, F-67034 Strasbourg Cedex 2, France

Received December 4, 2003; E-mail: bdonnio@ipcms.u-strasbg.fr

Abstract: The synthesis and the mesomorphic properties of several new main-chain liquid-crystalline dendrimers, thereafter designated as octopus dendrimers in accordance with their eight sidearms, are reported. In these dendritic systems, the arborescence is ensured by anisotropic segments, acting as branching cells with a double multiplicity, which are incorporated at every node of the dendritic architecture. In such a way, these compounds radically differ from the classical end-functionalized liquid-crystalline dendrimers, the most commonly reported systems. Following our previous report on purely homolithic systems, that is, the building blocks constituting the dendritic matrix are all identical, several heterolithic systems made of different anisotropic blocks have been prepared. The dendritic branches and corresponding dendrimers were synthesized using a modular construction. Polarized optical microscopy and X-ray diffraction studies showed that all of these new octopus dendrimers exhibit either smectic-like or columnar phases with novel morphologies, the nature of the mesophases depending on the number of terminal chains attached to the peripheral groups. The mesomorphism of these heterolithic dendrimers is discussed in terms of their intrinsic architecture and compared to the analogous homolithic octopus systems. Models for the molecular organizations within both the smectic and the columnar phases are proposed on the basis of small Bragg angle X-ray diffraction studies and are supported by molecular modelizations. Moreover, this study showed that the mesophase stability is very sensitive to the nature and to the mutual arrangement (the spatial location) of the mesogenic segments within the dendritic matrix, illustrating the intimate relationships existing between the mesomorphic properties and the molecular architecture of these dendrimers.

Introduction

Since their discovery in the late 1970s,[1] and the adjustments of perfectly controlled synthetic processes, dendrimers have led to the most impressive developments and rapidly expanding areas of current science.[2] This extraordinary enthusiasm was primarily caused by the intrinsic and unique molecular features of the dendrimers[2] and the possibility to generate numerous and original chemical architectures, offering new synthetic concepts and challenges for chemists[3] as well as raising several interesting theoretical questions.[4] Indeed, dendrons and dendrimers are a class of aesthetic, compartmentalized, practically monodisperse,

supermolecules possessing a regular and controlled branched topology,[2] with an exponential rate of growth as the generation number increases.[5] These features are the result of sophisticated genealogical directed syntheses consisting of controlled iterative methods involving successive and specific elementary steps (convergent or divergent directed sequential construction). The control of the ultimate molecular architecture (size and shape) can be modulated by the generation growth, the multiplicity of the branches, and the connectivity of the focal core. Research in this area has been further boosted by the appreciation of their uses as potentially interesting candidates in widespread applications.[6] Dendrimers may be used, when suitably functionalized, in biology as drug or gene delivery devices[7] due to their rough resemblance to some living components.[8] Or, alternatively, as ideal oligomeric substances, they may be designed as materials with precise functionalities in which molecular level information

(1) Tomalia, D. A.; Fréchet, J. M. *J. Polym. Sci., Part A: Polym. Chem.* **2002**, *40*, 2719−2728.
(2) (a) Tomalia, D. A.; Dupont Durst, H. *Top. Curr. Chem.* **1993**, *165*, 193−313. (b) Ardoin, N.; Astruc, D. *Bull. Soc. Chim. Fr.* **1995**, *132*, 875−909. (c) Newkome, G. R.; Moorefield, C. N.; Vögtle, F. *Dendritic Molecules: Concepts, Synthesis and Perspectives*; Wiley−VCH: Weinheim, 1996. (d) Ashton, P. R.; Boyd, S. E.; Brown, C. L.; Nepogodiev, S. A.; Meijer, E. W.; Peerlings, H. W. I.; Stoddart, J. F. *Chem.-Eur. J.* **1997**, *3*, 974−984. (e) Matthews, O. A.; Shipway, N.; Stoddart, J. F. *Prog. Polym. Sci.* **1998**, *23*, 1−56. (f) Newkome, G. R.; Moorefield, C. N.; Vögtle, F. *Dendrimers and Dendrons: Concepts, Synthesis and Perspectives*; Wiley−VCH: Weinheim, 2001. (g) Voit, B. I. *Acta Polym.* **1995**, *46*, 87−99.
(3) (a) Grayson, S. M.; Fréchet, J. M. *Chem. Rev.* **2001**, *101*, 3819−3867. (b) Hawker, C. J. *Adv. Polym. Sci.* **1999**, *147*, 113−160.
(4) (a) Tomalia, D. A.; Naylor, A. M.; Goddard, W. A., III. *Angew. Chem., Int. Ed. Engl.* **1990**, *29*, 138−175. (b) Tomalia, D. A. *Adv. Mater.* **1994**, *6*, 529−539.

(5) Feuerbacher, N.; Vögtle, F. *Top. Curr. Chem.* **1998**, *197*, 1−18.
(6) (a) Issberner, J.; Moors, R.; Vögtle, F. *Angew. Chem., Int. Ed. Engl.* **1994**, *33*, 2413−2420. (b) Dykes, G. M. *J. Chem. Technol. Biotechnol.* **2001**, *76*, 903−918.
(7) Boas, U.; Heegaard, P. M. H. *Chem. Soc. Rev.* **2004**, *33*, 43−63.
(8) (a) Astruc, D. *C. R. Acad. Sci. Paris Ser. II* **1996**, *322*, 757−766. (b) Uhrich, K. *Trends Polym. Sci.* **1997**, *5*, 388−393. (c) Smith, D. K.; Diederich, F. *Chem.-Eur. J.* **1998**, *4*, 1353−1361. (d) Hecht, S.; Fréchet, J. M. J. *Angew. Chem., Int. Ed.* **2001**, *40*, 74−91. (e) Cloninger, M. J. *Curr. Opin. Chem. Biol.* **2002**, *6*, 742−748.
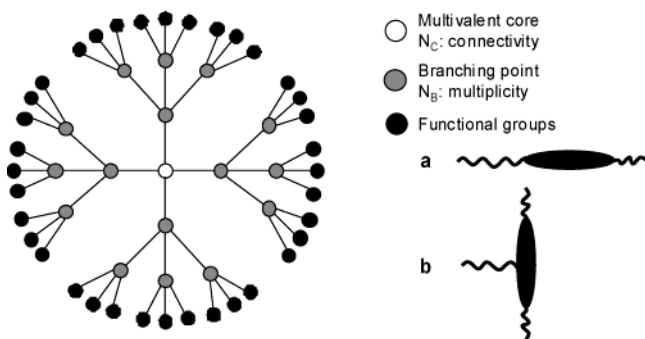
Figure 1. Schematic 2D representation of an end-group dendrimer of second generation with a 4-fold core connectivity ($N_C = 4$), and a ternary branch multiplicity ($N_B = 3$). The mesogen can be attached terminally or laterally to yield (a) end-on and (b) side-on LCDs.

is transferred from the initiator core to the periphery (or vice versa) with the expectation of complementary and synergic phenomena (i.e., induction of new properties) and/or cooperative effects (i.e., amplification of the existing properties).[9] Several excellent comprehensive review articles have emphasized many of the interesting assets of dendrimers.[2,4,5,10–12]

Molecular engineering of liquid crystals is also an important issue for controlling the self-assembling ability and the self-organizing process of single moieties into controlled nanostructures.[13] It was thus logical to functionalize such supermolecules to obtain liquid-crystalline materials[14] with the possibility to discover new types of mesophases and original morphologies.[15] So far, most studies have focused on side-group liquid-crystalline dendrimers (LCDs, Figure 1).[16] The overall structure of such side-group LCDs consists of a flexible branched network

emanating from a single multivalent initiator core and mesogenic units attached at the termini of the branches.[17–22] Induction of liquid-crystalline properties may simply be achieved by respecting these criteria,[17–22] although a few LCDs with nonmesogenic end-groups have been reported too.[23–25] Mesomorphism results essentially from both the enthalpic gain provided by anisotropic interactions and the strong tendency for microphase separation due to the chemical incompatibility between the flexible dendritic core and the terminal groups as in AB-block copolymers.[26] The structure of the mesogen as well as the topology of attachment to the core (end-on and side-on, Figure 1) determine the mesomorphism of the entire compound. Other subclasses of LCDs also include supramolecular dendromesogens,[27] shape-persistent,[28] metallodendrimers,[29] polypedic,[30] and fullerene-containing LCDs.[31] Let us note that the dendritic systems so far mentioned are distinct from hyperbranched polymers, often wrongly referred to as dendrimers, and are

(9) (a) Chow, H. F.; Mong, T. K. K.; Nongrum, M. F.; Wan, C. W. *Tetrahedron* **1998**, *54*, 8543–8660. (b) Archut, A.; Vögtle, F. *Chem. Soc. Rev.* **1998**, *27*, 233–240. (c) Fischer, M.; Vögtle, F. *Angew. Chem., Int. Ed.* **1999**, *38*, 884–905. (d) Inoue, K. *Prog. Polym. Sci.* **2000**, *25*, 453–571. (e) Vögtle, F.; Gestermann, S.; Hesse, R.; Schwierz, H.; Windisch, B. *Prog. Polym. Sci.* **2000**, *25*, 987–1041. (f) Adronov, A.; Fréchet, J. M. J. *Chem. Commun.* **2000**, 1701–1710. (g) Beletskaya, I. P.; Chuchurjukin, A. V. *Russ. Chem. Rev.* **2000**, *69*, 639–660.

(10) Synthesis of chiral systems: (a) Seebach, D.; Rheiner, P. B.; Greiveldinger, G.; Butz, T.; Sellner, H. *Top. Curr. Chem.* **1998**, *197*, 125–164. (b) Romagnoli, B.; Hayes, W. *J. Mater. Chem.* **2002**, *12*, 767–799.

(11) Metallodendrimers: (a) Constable, E. C. *Chem. Commun.* **1997**, 1073–1080. (b) Venturi, M.; Serroni, S.; Juris, A.; Campagna, S.; Balzani, V. *Top. Curr. Chem.* **1998**, *197*, 193–228. (c) Gorman, C. *Adv. Mater.* **1998**, *10*, 295–309. (d) Newkome, G. R.; He, E.; Moorefield, C. N. *Chem. Rev.* **1999**, *99*, 1689–1746. (e) Hearshaw, M. A.; Moss, J. R. *Chem. Commun.* **1999**, 1–8. (f) Stoddart, F. J.; Welton, T. *Polyhedron* **1999**, *18*, 3575–3591. (g) Cuadrado, I.; Morán, M.; Casado, C. M.; Alonso, B.; Losada, J. *Coord. Chem. Rev.* **1999**, *193–195*, 395–445.

(12) Heteroatom-based dendrimers: (a) Majoral, J. P.; Caminade, A. M. *Top. Curr. Chem.* **1998**, *197*, 79–124. (b) Majoral, J. P.; Caminade, A. M. *Chem. Rev.* **1999**, *99*, 845–880. (c) Frey, H.; Lach, C.; Lorenz, K. *Adv. Mater.* **1998**, *10*, 279–293. (d) Frey, H.; Schlenk, C. *Top. Curr. Chem.* **2000**, *210*, 69–129. (e) Lang, H.; Lühmann, B. *Adv. Mater.* **2001**, *13*, 1523–1540.

(13) (a) Zeng, F.; Zimmerman, S. C. *Chem. Rev.* **1997**, *97*, 1681–1712. (b) Narayanan, V. V.; Newkome, G. R. *Top. Curr. Chem.* **1998**, *197*, 19–77. (c) Constable, E. C.; Housecroft, C. E. *Chimia* **1998**, *52*, 533–538. (d) Emrick, T.; Fréchet, J. M. J. *Curr. Opin. Colloid Interface Sci.* **1999**, *4*, 15–23. (e) Smith, D. K.; Diederich, F. *Top. Curr. Chem.* **2000**, *210*, 183–227.

(14) (a) Goodby, J. W.; Mehl, G. H.; Saez, I. M.; Tuffin, R. P.; Mackenzie, G.; Auzély-Velty, R.; Benvegnu, T.; Plusquellec, D. *Chem. Commun.* **1998**, 2057–2070. (b) Goodby, J. W. *Curr. Opin. Solid State Mater. Sci.* **1999**, *4*, 361–368. (c) Ponomarenko, S. A.; Boiko, N. I.; Shibaev, V. P. *Polym. Sci., Ser. A* **2001**, *43*, 1–45.

(15) (a) Demus, D. *Liq. Cryst.* **1989**, *5*, 75–110. (b) Tschierske, C. *Prog. Polym. Sci.* **1996**, *21*, 775–852. (c) Tschierske, C. *J. Mater. Chem.* **1998**, *8*, 1485–1508. (d) Pelzl, G.; Diele, S.; Weissflog, W. *Adv. Mater.* **1999**, *11*, 707–724. (e) Tschierske, C. *J. Mater. Chem.* **2001**, *11*, 2647–2671. (f) Tschierske, C. *Curr. Opin. Colloid Interface Sci.* **2002**, *7*, 69–80. (g) Tschierske, C. *Annu. Rep. Prog. Chem., Sect. C* **2001**, *97*, 191–267. (h) Cheng, X.; Prehm, M.; Das, M. K.; Kain, J.; Baumeister, U.; Diele, S.; Dag, L.; Blume, A.; Tschierske, C. *J. Am. Chem. Soc.* **2003**, *125*, 10977–10996.

(16) This terminology is used by analogy to side-chain liquid crystal polymers.

(17) Polypropyleneimines LCDs (DAB): (a) Stebani, U.; Lattermann, G. *Adv. Mater.* **1995**, *7*, 578–581. (b) Seitz, M.; Plesnivy, T.; Schimossek, K.; Edelmann, M.; Ringsdorf, H.; Fischer, H.; Uyama, H.; Kobayashi, S. *Macromolecules* **1996**, *29*, 6560–6574. (c) Baars, M. W. P. L.; Söntjens, S. H. M.; Fischer, H. M.; Peerlings, H. W. I.; Meijer, E. W. *Chem.-Eur. J.* **1998**, *4*, 2456–2466. (d) Yonetake, K.; Masuko, T.; Morishita, T.; Suzuki, K.; Ueda, M.; Nagahata, R. *Macromolecules* **1999**, *32*, 6578–6586.

(18) Polyamidoamines LCDs (PAMAM): (a) Barberá, J.; Marcos, M.; Serrano, J. L. *Chem.-Eur. J.* **1999**, *5*, 1834–1840. (b) Marcos, M.; Giménez, R.; Serrano, J. L.; Donnio, B.; Heinrich, B.; Guillon, D. *Chem.-Eur. J.* **2001**, *7*, 1006–1013. (c) Donnio, B.; Barberá, J.; Giménez, R.; Guillon, D.; Marcos, M.; Serrano, J. L. *Macromoelcules* **2002**, *35*, 370–381.

(19) Polysiloxanes LCDs: Ponomarenko, S. A.; Rebrov, E. A.; Boiko, N. I.; Vasilenko, N. G.; Muzafarov, A. M.; Freidzon, Y. S.; Shibaev, V. P. *Polym. Sci., Ser. A* **1994**, *36*, 896–901.

(20) Polycarbosilanes LCDs: (a) Ponomarenko, S. A.; Rebrov, E. A.; Bobronsky, Y.; Boiko, N. I.; Muzafarov, A. M.; Shibaev, V. P. *Liq. Cryst.* **1996**, *21*, 1–12. (b) Lorenz, K.; Hölter, D.; Mühlhaupt, R.; Frey, H. *Adv. Mater.* **1996**, *8*, 414–416. (c) Ryumtsev, E. I.; Evlampieva, N. P.; Lezov, A. V.; Ponomarenko, S. A.; Boiko, N. I.; Shibaev, V. P. *Liq. Cryst.* **1998**, *25*, 475–476. (d) Ponomarenko, S. A.; Rebrov, E. A.; Boiko, N. I.; Muzafarov, A. M.; Shibaev, V. P. *Polym. Sci., Ser. A* **1998**, *40*, 763–774. (e) Ponomarenko, S. A.; Boiko, N. I.; Shibaev, V. P.; Richardson, R. M.; Whitehouse, I. J.; Rebrov, E. A.; Muzafarov, A. M. *Macromolecules* **2000**, *33*, 5549–5558.

(21) Polycarbosilazane LCDs: Elsässer, R.; Mehl, G.; Goodby, J. W.; Veith, M. *Angew. Chem., Int. Ed.* **2001**, *40*, 2688–2690.

(22) LCDs with polyether cores: (a) Busson, P.; Ihre, H.; Hult, A. *J. Am. Chem. Soc.* **1998**, *120*, 9070–9071. (b) Busson, P.; Örtegren, J.; Ihre, H.; Gedde, U. W.; Hult, A.; Andersson, G. *Macromolecules* **2001**, *34*, 1221–1229. (c) Busson, P.; Örtegren, J.; Ihre, H.; Gedde, U. W.; Hult, A.; Andersson, G.; Eriksson, A.; Lindgren, M. *Macromolecules* **2002**, *35*, 1663–1671.

(23) Lorenz, K.; Frey, H.; Stühn, B.; Mülhaupt, R. *Macromolecules* **1997**, *30*, 6860–6868.

(24) Cameron, J. H.; Facher, A.; Latterman, G.; Diele, S. *Adv. Mater.* **1997**, *9*, 398–403.

(25) Tsiourvas, D.; Stathopoulou, K.; Sideratou, Z.; Paleos, C. M. *Macromolecules* **2002**, *35*, 1746–1750.

(26) Hamley, I. W. *The Physics of Block-Copolymers*; Oxford University Press: Oxford, 1998.

(27) (a) Balagurusamy, V. S. K.; Ungar, G.; Percec, V.; Johansson, G. *J. Am. Chem. Soc.* **1997**, *119*, 1539–1555. (b) Hudson, S. D.; Jung, H. T.; Percec, V.; Cho, W. D.; Johansson, G.; Ungar, G.; Balagurusamy, U. S. K. *Science* **1997**, *278*, 449–452. (c) Percec, V.; Schlueter, D.; Ungar, G.; Cheng, S. Z. D.; Zhang, A. *Macromolecules* **1998**, *31*, 1745–1762. (d) Percec, V.; Cho, W. D.; Mosier, P. E.; Ungar, G.; Yeardley, D. J. P. *J. Am. Chem. Soc.* **1998**, *120*, 11061–11070. (e) Hudson, S. D.; Jung, H. T.; Kewsuwan, P.; Percec, V.; Cho, W. D. *Liq. Cryst.* **1999**, *26*, 1493–1499. (f) Ungar, G.; Percec, V.; Holerca, M. N.; Johansson, G.; Heck, J. A. *Chem.-Eur. J.* **2000**, *6*, 1258–1266. (g) Percec, V.; Cho, W. D.; Ungar, G.; Yeardley, D. J. P. *Angew. Chem., Int. Ed.* **2000**, *39*, 1597–1602. (h) Percec, V.; Cho, W. D.; Möller, M.; Prokhorova, S. A.; Ungar, G.; Yeardley, D. J. P. *J. Am. Chem. Soc.* **2000**, *122*, 4249–4250. (i) Percec, V.; Cho, W. D.; Ungar, G. *J. Am. Chem. Soc.* **2000**, *122*, 10273–10281. (j) Percec, V.; Cho, W. D.; Ungar, G.; Yeardley, D. J. P. *J. Am. Chem. Soc.* **2001**, *123*, 1302–1315. (k) Ungar, G.; Liu, Y.; Zeng, X.; Percec, V.; Cho, W. D. *Science* **2003**, *299*, 1208–1211.

(28) (a) Moore, J. S. *Acc. Chem. Res.* **1997**, *30*, 13377–13394. (b) Pesak, D. J.; Moore, J. S. *Angew. Chem., Int. Ed. Engl.* **1997**, *36*, 1636–1639. (c) Meier, H.; Lehmann, M. *Angew. Chem., Int. Ed.* **1998**, *37*, 643–645. (d) Meier, H.; Lehmann, M.; Kolb, U. *Chem.-Eur. J.* **2000**, *6*, 2462–2469.

(29) (a) Stebani, U.; Lattermann, G.; Wittenberg, M.; Wendorff, J. H. *Angew. Chem., Int. Ed. Engl.* **1996**, *35*, 1858–1861. (b) Barberá, J.; Marcos, M.; Omenat, A.; Martínez, J. I.; Alonso, P. J. *Liq. Cryst.* **2000**, *27*, 255–262. (c) Deschenaux, R.; Serrano, E.; Levelut, A. M. *Chem. Commun.* **1997**, 1577–1578.
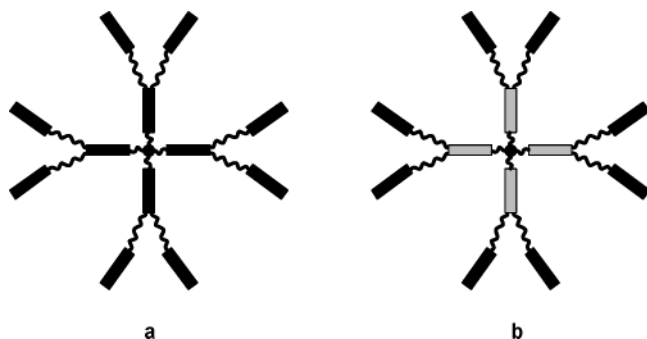
Figure 2. Schematic 2D representation of (a) homolithic and (b) heterolithic main-chain liquid-crystalline octopus dendrimers.

characterized by randomly branched structures with a high degree of branching and broad molecular weight distributions.[32] Adequately functionalized, they have also been found to form original mesomorphic systems.[33,34]

We have recently reported on a new family of LCDs, affectionately named octopus LCDs[35] in accordance with their eight arms (Figure 2), for which the arborescence is ensured by anisometric segments acting as branching cells, incorporated at every node of the dendritic architecture by modular construction.[36] Due to the presence of anisotropic groups at every level of the dendritic hierarchy (and thus of additional intermesogen interactions), the dendrimers are forced to adopt constrained and regular structures, radically differing in this respect from their side-chain homologues. For this study,[35] the building blocks constituting the dendritic matrix were stilbene groups, and as such these octopus dendrimers were described as homolithic. The principles of the modular construction can be applied for the preparation of co-dendrimers made of two basic building bricks (heterolithic systems), which can be arranged independently in a controlled, alternated manner (Figure 2). The ability of such polyfunctional and discrete dendritic structures to self-assemble into mesophases may be an attractive strategy in the field of materials science for the elaboration of multicomponent nanosize objects. In this paper, the design and the synthetic methodology of new homolithic and heterolithic octopus dendrimers are presented. The mesomorphic behavior is discussed

as a function of the number of peripheral alkoxy chains, and, due to the multicomponent nature of the compounds, the effects of the anisotropic moieties as well as their spatial location and mutual arrangement within the dendritic scaffolds will be emphasized. A model accounting for the molecular organization of these octopus dendrimers into the smectic and columnar phases is proposed on the basis of X-ray diffraction studies and molecular modelizations.

Synthesis

Synthetic Methodology. The anisotropic units selected for this work were stilbene- and tolane-based moieties that were chosen not only for the versatility of their chemistry, their ease of derivatization, and their good thermal stability, but also for the poor mesogenic character of the parent di-4,4′-alkoxy homologues.[37] This latter point was important to test whether mesomorphism could be induced solely by the self-assembling process of the dendrimers, on one hand, and to be able to monitor with a great sensitivity the effects of small structural variations on the mesomorphic properties of the resultant dendrimers, on the other hand.

All of these new main-chain dendrimers were prepared by modular construction (Schemes 1–3).[35] The dendritic branches were constructed in a two-stage procedure. The first stage involved the simultaneous preparation of the various constitutive building bricks, including both the difunctionalized AB$_2$-type stilbene (**4**) and tolane (**10**) derivatives (Scheme 1) and the terminal functional "stilbenol" (**13**) and "tolanol" groups (**16a,b**) (Scheme 2). In the second stage of the procedure, these building blocks were assembled selectively together to produce the desired focal point functionalized dendrons (Scheme 3, acids **17a–e**). As for the final dendrimers, they were obtained by a convergent method consisting of the chemical coupling of these acidic branches, through amino linkage, to a small tetravalent core unit, tetra-amino core *N,N,N′,N′*-tetrakis(3-aminopropyl)-1,4-butanediamine (DAB, Generation 1.0) (Scheme 3, **19a–e**).

Preparation of the Internal Branching Subunits, 4 and 10. The internal branching units, **4** and **10**, were prepared in several steps using standard chemical reactions as shown in Scheme 1. For the preparation of **4**, the commercially available starting material, 3,5-dimethoxy benzaldehyde, was almost quantitatively converted into the corresponding styrene (**1**) by a Wittig reaction. The coupling of this styrene derivative with the appropriate ethyl 4-iodobenzoate via a palladium-catalyzed Heck reaction then produced the dimethoxy stilbene ester derivative, **2**, also in good yields. The dihydroxy compound **3** was obtained in two successive steps including first the demethylation with BBr$_3$, immediately followed by the re-esterification of the acid function because the ester group did not survive the demethylation. Finally, bromoundecanol was grafted to the free hydroxyl groups of **3** by a Mitsunobu etherification to yield the prefunctionalized internal core moiety, **4**. The analogous tolane compound **10** was prepared in seven steps. It first consisted of the conversion of the commercially available 3,5-dimethoxy aniline into 3,5-dimethoxy iodobenzene (**5**) by a Sandmeyer reaction. Such an iodo derivative was then coupled with trimethylsilylacetylene via a Sonogashira coupling reaction to yield **6**, which was deprotected to give the true

(30) (a) Mehl, G. H.; Saez, I. M. *Appl. Organomet. Chem.* **1999**, *13*, 261–272. (b) Saez, I. M.; Goodby, J. W. *Liq. Cryst.* **1999**, *26*, 1101–1105. (c) Saez, I. M.; Goodby, J. W. *Chem.-Eur. J.* **2003**, *9*, 4869–4877. (d) Campidelli, S.; Eng, C.; Saez, I. M.; Goodby, J. W.; Deschenaux, R. *Chem. Commun.* **2003**, 1520–1521. (e) Saez, I. M.; Goodby, J. W. *J. Mater. Chem.* **2003**, *13*, 2727–2739.

(31) (a) Dardel, B.; Deschenaux, R.; Even, M.; Serrano, E. *Macromolecules* **1999**, *32*, 5193–5198. (b) Chuard, T.; Dardel, B.; Deschenaux, R.; Even, M. *Carbon* **2000**, *38*, 1573–1576. (c) Campidelli, S.; Deschenaux, R. *Helv. Chim. Acta* **2001**, *84*, 589–593. (d) Dardel, B.; Guillon, D.; Heinrich, B. *J. Mater. Chem.* **2001**, *11*, 2814–2831. (e) Deschenaux, R.; Chuard, T.; Deschenaux, R. *J. Mater. Chem.* **2002**, *12*, 1944–1951.

(32) (a) Flory, P. J. *Principles of Polymer Chemistry*; Cornell University Press: Ithaca, NY, 1953. (b) Kim, Y. H. *J. Polym. Sci., Part A: Polym. Chem.* **1998**, *36*, 1685–1698. (c) Frey, H.; Hölter, D. *Acta Polym.* **1999**, *50*, 67–76. (d) Hult, A.; Johansson, M.; Malmström, E. *Adv. Polym. Sci.* **1999**, *143*, 1–34.

(33) Main-chain systems: (a) Percec, V.; Kawasumi, M. *Macromolecules* **1992**, *25*, 3843–3850. (b) Bauer, S.; Fischer, H.; Ringsdorf, H. *Angew. Chem., Int. Ed. Engl.* **1993**, *32*, 1589–1592. (c) Percec, V.; Chu, P.; Kawasumi, M. *Macromolecules* **1994**, *27*, 4441–4453. (d) Hanh, S. W.; Yun, S. Y. K.; Jin, J. I.; Han, O. H. *Macromolecules* **1998**, *31*, 6417–6425.

(34) Side-chain systems: Sunder, A.; Quincy, M. F.; Mülhaupt, R.; Frey, H. *Angew. Chem., Int. Ed.* **1999**, *38*, 2928–2930.

(35) Gehringer, L.; Guillon, D.; Donnio, B. *Macromolecules* **2003**, *36*, 5593–5601.

(36) The concept and the compounds remain very different from the so-called willow-like LCDs reported some years (a) Percec, V.; Chu, P.; Ungar, G.; Zhou, J. *J. Am. Chem. Soc.* **1995**, *117*, 11441–11454. (b) Li, J. L.; Crandall, K. A.; Chu, P.; Percec, V.; Petschek, R. G.; Rosenblatt, C. *Macromolecules* **1996**, *29*, 7813–7819.

(37) Demus, D.; Demus, H.; Zaschke, H. *Flüssige Kristalle in Tabellen*; VEB Deutscher Verlag für Grundstoffindustrie: Leipzig, 1974.

Scheme 1. Preparation of the Internal Branching Units **4** and **10**
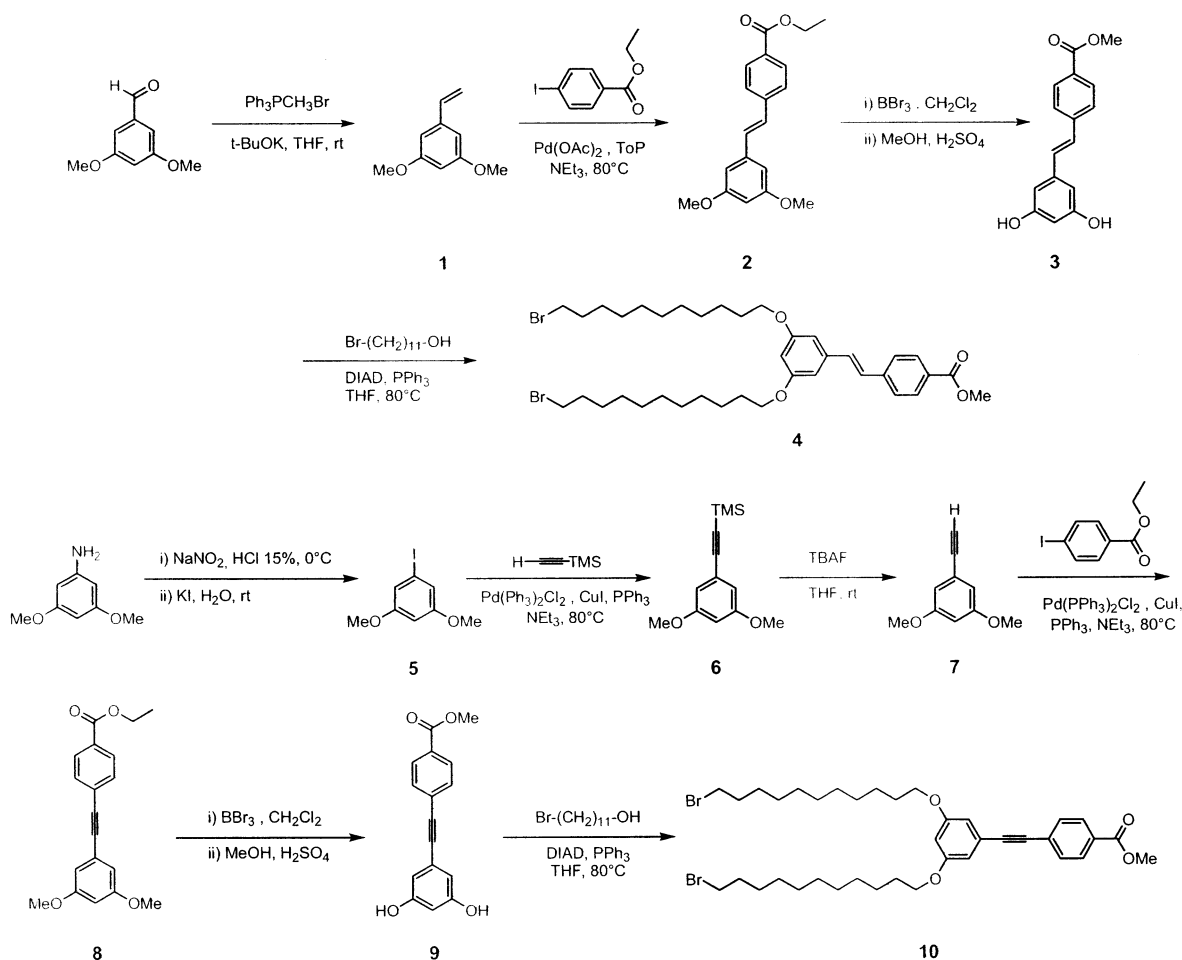
Scheme 2. Preparation of the Terminal Groups **7a**−**d**
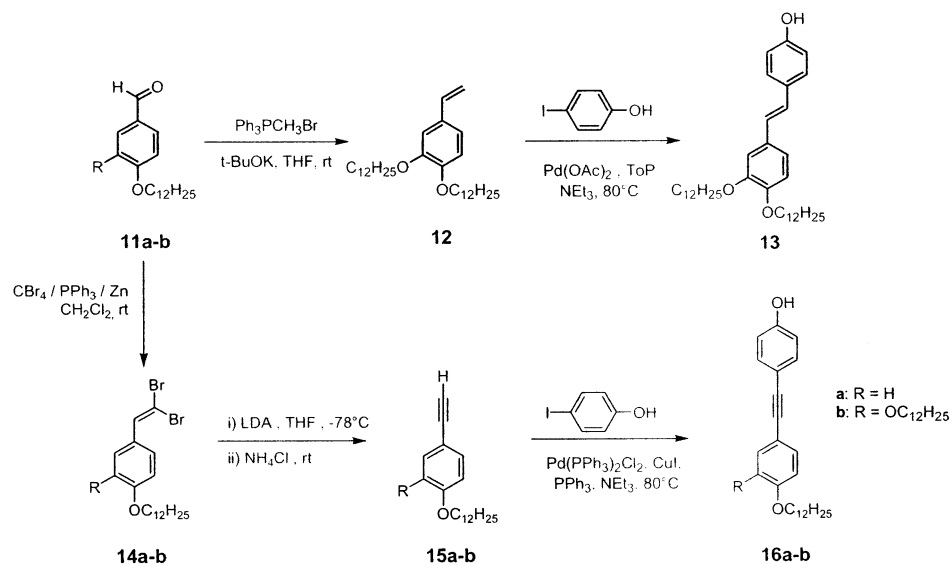
acetylene derivative **7**. The tolane species **8** was obtained by a second Sonogashira coupling between **7** and ethyl 4-iodobenzoate. Compounds **9** and **10** were finally obtained using exactly the same procedures as were used for the preparation of **3** and **4**, respectively.

Preparation of the Terminal Groups, 13 and 16. Compounds **13** and **16** were prepared from the same alkoxy-

substituted benzaldehydes. Mono- and 3,4-dialkoxytolanoidelike moieties (**16a,b**) were prepared by identical synthetic methods, including the prior conversion of the appropriate alkoxybenzaldehydes into the corresponding dibromo vinylic compounds (**14a,b**) by the Corey−Fuchs procedure, which under basic conditions was transformed into the true acetylenic derivatives **15a,b**. **16a,b** were obtained by a Sonogashira

Scheme 3. Preparation of the Dendritic Branches (Acids **17a**−**f**) and the Corresponding Octopus Dendrimers **19a**−**f**
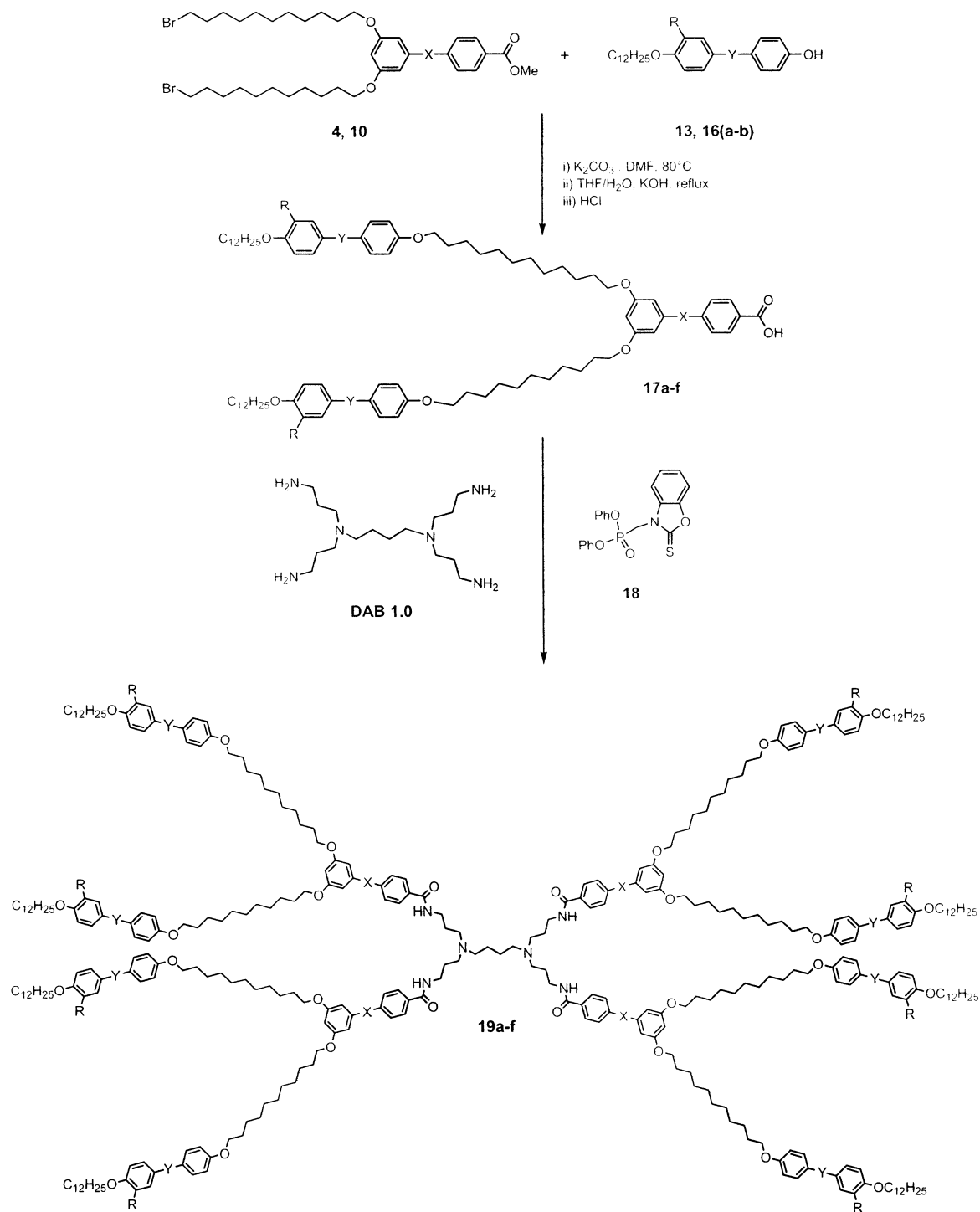
	a	**b**	**c**	**d**	**e**	**f**
R	H	$OC_{12}H_{25}$	H	$OC_{12}H_{25}$	$OC_{12}H_{25}$	$OC_{12}H_{25}$
X	C≡C	C≡C	C=C	C=C	C≡C	C=C
Y	C≡C	C≡C	C≡C	C≡C	C=C	C=C

coupling between **15a,b** and iodophenol. The 3,4-dialkoxystil-benoide-like moiety, **13**, was obtained by the conversion of the dialkoxybenzaldehyde (**11**) into the corresponding styrene (**12**), followed in the next step by its coupling to iodophenol under palladium-catalyzed Heck reaction conditions (Scheme 2).

Preparation of the Precursory Acid Dendrons 17 and Corresponding Octopus 19. The esters, precursors of the various acidic branches **17**, were obtained by straightforward double alkylation reactions between the internal unit **4** or **10** and the appropriate stilbene (**13**) or tolane derivatives (**16a,b**);

their subsequent hydrolysis yielded the desired acids **17a−f** (Scheme 3). The targeted octopus dendrimers (**19a−f**) were obtained by reaction of the acid **17a−f** with DAB, Generation 1.0, the acid function being activated by diphenyl(2,3-dihydro-2-thioxo-3-benzoxazolyl)phosphonate, **18**.[38] Note that the dendron **17f**, and the corresponding dendrimer **19f**, were already prepared.[35] Unfortunately, due to solubility reasons, the acid monodendrons and corresponding dendrimers having a single-chain stilbene as end-groups (**17**, **19**: Y = C=C, X = C=C, C≡C, R = H) could not be synthesized.

All of the final compounds were isolated as air-stable crystalline solids (except **19a** obtained as a waxy material) and were soluble in most organic solvents. The acidic arms were purified by repeated crystallizations in petroleum ether, and the dendrimers were purified by flash chromatography.

Structural Characterization of the Octopus Dendrimers. The purity and characterization of the precursory dendritic acids were determined by a combination of thin-layer chromatography (TLC), ^{1}H and ^{13}C NMR spectroscopy, and MALDI-TOF mass spectroscopy, and the final dendrimers were analyzed by additional elemental analysis and SEC. The purity of all intermediary compounds was only checked by ^{1}H NMR spectroscopy and TLC. In all cases, the results were in good agreement with the proposed structures. The absolute molecular weights were given by MALDI-TOF MS, which showed the correct molecular peaks with additional lower mass fragments, in small amount, which did not correspond to intermediate compounds. The SEC analysis showed a monomodal molecular weight distribution, with polydispersity indices close to unity, meaning that the dendrimers were monodisperse. All of these data, as well as the detailed synthetic procedures, have been deposited in the Supporting Information.

Results and Discussion

The thermal behavior of the acid monodendrons and of the dendrimers was investigated by three complementary techniques: polarized optical microscopy (POM), differential scanning calorimetry (DSC), and small-angle X-ray diffraction (XRD).

Optical and Thermal Studies by POM, TGA, and DSC. The liquid-crystalline behavior of all of the dendrimers was probed by the observation under polarized microscope of optical textures showing homogeneous, birefringent, and fluid domains, coalescing on an increase in the temperature; the presence of large homeotropic domains pointed either to orthogonal-type smectic phases (SmA or SmB) or to a columnar hexagonal phase (Col$_h$). In contrast, none of the precursor acids, except **17e**, was mesomorphic. Some general trends can be immediately deduced from these observations. On the basis of cylindrical domains or focal-conic-like textures being observed in some cases and not in other cases, and of the differences in viscosity, two groups of compounds could be distinguished, one set consisting of **19a** and **19c**, and the other set made of **19b**, **19d,e**. Dendrimers with peripheral groups having one terminal chain only (**19a**, **19c**) were mesomorphic at or near room temperature, up to 121 °C (**19a**) or 140 °C (**19c**); the crystalline phase of **19c** was not recovered after the first heating. In contrast, the compounds with two terminal chains per end-groups (**19b**, **19d,e**) melted into a

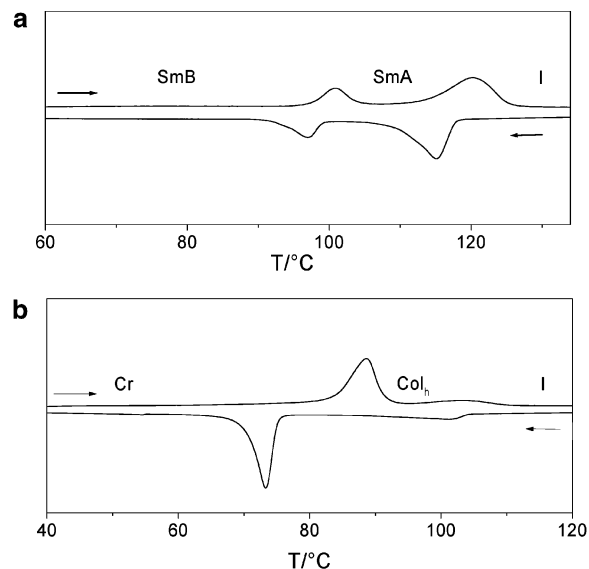(38) Ueda, M.; Kameyama, A.; Hashimoto, K. *Macromolecules* **1988**, *21*, 19−24.

Figure 3. Representative DSC traces: (a) **19a** and (b) **19e**.

mesophase at higher temperatures (ca. 80−90 °C) and cleared at or above 100 °C; only one compound (**19b**) exhibited a monotropic mesophase (the mesophase appeared on cooling from the isotropic liquid). Comparing octopus having identical dendritic cores, **19a,b** and **19c,d**, respectively, we observed an important reduction of the mesophase stability with the doubling of the terminal aliphatic chains number.

No conclusive and unequivocal mesophase assignment could be given by this technique of characterization because no typical and recognizable optical textures were obtained. However, as compared to the homolithic stilbene dendrimers reported recently,[35] it is safe to assign a columnar phase for compounds **19b**, **19d,e**, consistent with the number of terminal chains grafted to the peripheral groups, and to predict a smectic-like behavior for **19a** and **19c**. Some optical textures have been deposited in the Supporting Information.

Confirming the results of the microscopic observations, several first-order transitions were detected by DSC at corresponding temperatures. Most of the dendrimers exhibited complicated and nonexploitable DSC traces during the first heating scan, a common situation in macromolecular systems. However, on subsequent heating−cooling cycles, more simple and perfectly reproducible thermograms were obtained as shown by two representative dendrimers of each group (Figure 3). This good thermal stability was also confirmed by thermogravimetry showing a loss-weight of less than 5% detected above 200 °C, with no more degradation observed up to 300 °C, well above the transition into the isotropic liquid. In agreement with POM, the DSC traces consisted of crystal-to-mesophase transformations (**19b**, **19c−e**) and of mesophase-to-isotropic liquid transitions (Figure 3, Table 1). In the case of **19a** and **19c**, an additional enthalpy change was seen, likely corresponding to a mesophase-to-mesophase transformation (Figure 3a). The transition temperatures of the acids and dendrimers are gathered in Table 1. The fairly large values of the transitions' enthalpies were at first surprising, but were probably due to long and complicated reorganization processes, to the numerous π−π intermolecular interactions, and to the important volume of aliphatic chains per mesogenic group and dendrimer. This thermodynamic feature will be discussed later. On cooling,

Table 1. Thermal Behavior of the Dendritic Branches and Octopus Dendrimers and X-ray Characterization of the Mesophases[a]

compound	transition temperatures/°C	d_{meas}/Å	I	00l	hk	d_{calc}/Å	mesophase parameters measured at T	molecular volume at T (V_{mol})	N
17a	Cr 150 I								
17b	Cr 103 I								
17c	Cr 155 I								
17d	Cr 125 I								
17e	Cr 111 (137.8[b]) Col$_h$ 124 (6.1[b]) I[c]	58.9	VS		10	58.9	$T = 115$ °C	$V_{mol} = 3000$ Å^3	6.0
		33.7	S		11	34.0	$a = 68.0$ Å		
		29.7	S		20	29.45	$S = 4005$ Å^2		
		4.5	br		h		$V_{cell} = 18\,090$ Å^3		
17f	Cr 146 I								
19a	SmB 101 (49.0[b]) SmA 121 (127.4[b]) I[c]	107.1	VS	001		106.9	$T = 80$ °C	$V_{mol} = 9545$ Å^3	
		53.5	S	002		53.45	$d = 106.9$ Å		
		35.5	S	003		35.6	$A_M = 89.3$ Å^2		
		4.5	br	h			$a_m = 22.3$ Å^2		
		4.3	sh						
		97.4	VS	001		97.3	$T = 110$ °C	$V_{mol} = 9750$ Å^3	
		48.7	S	002		48.65	$d = 97.3$ Å		
		32.4	S	003		32.45	$A_M = 100.2$ Å^2		
		4.5	br	h			$a_m = 25.05$ Å^2		
19b	Cr 78 (Col$_h$ 75) I[d]	78.4	VS		10	77.8	$T = 75$ °C	$V_{mol} = 12\,055$ Å^3	2.6
		44.3	M		11	44.9	$a = 89.8$ Å		
		29.6	S		21	29.4	$S = 6990$ Å^2		
		4.5	br		h		$V_{cell} = 31\,450$ Å^3		
19c	Cr 65 (165.7[b]) SmB 110 (50.5[b]) SmA 140 (144.5[b]) I	104.0	VS	001		104.0	$T = 90$ °C	$V_{mol} = 9625$ Å^3	
		52.1	S	002		52.0	$a = 104.0$ Å		
	SmB 109 (53.1[b]) SmA 132 (127.3[b]) I[e]	34.6	S	003		34.7	$A_M = 92.6$ Å^2		
		4.5	br	h			$a_m = 23.15$ Å^2		
		4.3	sh						
		102.0	VS	001		101.8	$T = 120$ °C	$V_{mol} = 9830$ Å^3	
		50.9	S	002		50.9	$a = 101.8$ Å		
		33.9	S	003		33.9	$A_M = 96.6$ Å^2		
		4.5	br	h			$a_m = 24.15$ Å^2		
19d	Cr 82 (200.4[b]) Col$_h$ 98 (44.0[b]) I[e]	84.0	VS		10	84.2	$T = 90$ °C	$V_{mol} = 12\,200$ Å^3	3.0
		48.9	M		11	48.6	$a = 97.2$ Å		
		42.3	M		20	42.1	$S = 8170$ Å^2		
		31.6	S		21	31.8	$V_{cell} = 36\,750$ Å^3		
		4.5	br		h				
19e	Cr 88 (249.4[b]) Col$_h$ 110 (52.6[b]) I[e]	82.0	VS		10	81.7	$T = 105$ °C	$V_{mol} = 12\,345$ Å	2.8
		47.2	S		11	47.2	$a = 94.3$ Å		
		40.7	S		20	40.85	$S = 7705$ Å^2		
		31.0	S		21	30.9	$V_{cell} = 34\,600$ Å^3		
		23.5	M		22	23.6			
		22.7	M		31	22.65			
		4.5	br		h				
19f	Cr 95 (227[b]) Col$_h$ 132 (17.8[b]) I[e,f]	82.45	VS		10	82.45	$T = 100$ °C	$V_{mol} = 12\,300$ Å^3	2.9
		47.55	S		11	47.6	$a = 95.2$ Å		
		41.4	M		20	41.2	$S = 7850$ Å^2		
		31.1	S		21	31.15	$V_{cell} = 35\,320$ Å^3		
		23.8	M		22	23.8			
		4.5	br		h				

[a] d_{meas} and d_{calc} are the measured and calculated diffraction spacings (d_{calc} is deduced from the following mathematical expressions: $\langle d_{001} \rangle = 1/N_l \, (\sum_l d_{00l} \cdot l)$, where N_l is the number of 00l reflections for the SmA and SmB phases; $\langle d_{10} \rangle = 1/N_{hk} (\sum_{h,k} d_{hk} \cdot \sqrt{h^2+k^2+hk})$, where N_{hk} is the number of hk reflections for the Col$_h$ phase); I is the intensity of the reflection (VS, very strong; S, strong; M, medium; br, broad; sh, sharp); 00l and hk are the indexations of the reflections corresponding to the smectic and Col$_h$ phases, respectively; d is the smectic periodicity ($d = \langle d_{001} \rangle$); A_M is the molecular area ($A_M = V_{mol}/d$); and a_m is the area of one mesogenic unit ($a_m = A_M/4$); a is the lattice parameter of the Col$_h$ phase ($a = 2/\sqrt{3} \langle d_{10} \rangle$); S is the lattice area ($S = a \langle d_{10} \rangle$); V_{cell} is the volume of the hexagonal cell ($h \cdot S$), that is, a slice of column h-thick; the molecular volume is defined as $V_{mol} = (M/\rho 0.6022)(V_{CH_2}(T)/V_{CH_2}(T_0))$; M is the molecular weight; $V_{CH_2}(T) = 26.5616 + 0.02023T$ (T in °C, $T_0 = 22$ °C); ρ is the volume mass (1 g cm^{-3}); N is the number of molecules per V_{cell} ($N = V_{cell}/V_{mol}$); Cr, crystalline phase; I, isotropic liquid; SmB and SmA, smectic B and smectic A phases; Col$_h$, hexagonal columnar phase. [b] ΔH (kJ mol^{-1}). [c] Identical first and second heatings. [d] Determined on cooling. [e] Second heating. [f] Data reported in ref 35.

crystallization was systematically observed for **19b**, **19d,e** (as for **19f**), whereas it was absent for **19a** and **19c**, which retained the low-temperature mesophase down to room temperature.

Structural Investigation of the Mesophases by Small-Angle X-ray Diffraction. Identification and unequivocal assignment of the mesophases were finally achieved by small-angle X-ray diffraction on powder samples. Qualitatively similar X-ray patterns were obtained for structurally related dendrimers, that is, **19a** and **19c**, on one hand, and **19b**, **19d,e**, on the other hand.

(a) The Smectic-Like Phases. The smectic nature of the mesophases suggested by POM for **19a** and **19c** was eventually confirmed by X-ray diffraction; both compounds exhibited exactly the same X-ray patterns. The powder X-ray patterns recorded in the temperature intervals delimited by DSC exhibited a set of three sharp and equidistant small-angle reflections in the ratio 1:2:3 (Table 1), corresponding to the smectic layering of the molecules, and a diffuse scattering halo in the wide angle region, centered around 4.5 Å, associated to the liquidlike order
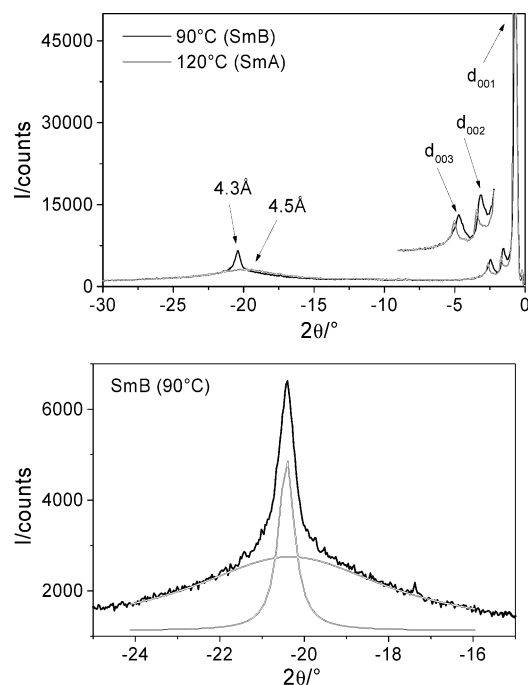
Figure 4. (a) X-ray pattern of **19c** at 90 °C (SmB) and 120 °C (SmA). (b) Decomposition of the wide angle signal into a sum of two functions.

of the molten aliphatic chains and rigid parts (Figure 4a). As for the lower-temperature phase, an additional sharp peak (4.3 Å) was seen, still in association with the diffuse scattering (Figure 4b), pointing to a long-range, hexatic order within the smectic layer. Thus, on the basis of these X-ray patterns, the high-temperature phase can be assigned as a disordered smectic phase (i.e., SmA or SmC), whereas the other, low-temperature, phase due to the extra in-layer order can be assigned as a hexatic smectic phase (i.e., SmB, SmF, or SmI). The observation by POM of large homeotropic areas indicates orthogonal smectic phases, and they can safely be assigned as SmA and SmB phases for the high- and low-temperature mesophases, respectively.

In a first approximation, one can realistically assume an elongated conformation for the dendrimer, where the rigid parts are collinear to the layer normal. Indeed, to allow the formation of lamellar mesophases, the overall molecular structure should adopt such a parallel conformation, with the elementary mesogenic units arranged in a pseudo-parallel fashion, with necessarily half the mesogenic units (i.e., four in the present case) extending up and the other half extending down the molecular center.[18] As such, the molecular model of the smectic layer consists of a tetragonal periodic cell in which the cross section was set to match roughly the molecular area of four mesogens in a SmA phase (10×10 Å^2). The third parameter of the cell was fixed to 150 Å, much longer than the length of the fully extended dendrimer to simulate a single layer and to allow the molecules to expand or shrink freely. A molecular dynamics (MD) simulation was then performed on this model to evaluate the dendrimer conformation within the smectic layer. The result of these calculations is represented by the molecular snapshot in Figure 5, and the estimated molecular length (ca. $90-100$ Å) was found to be in very good agreement with periodicities measured by XRD (ca. 100 Å).

To verify the pertinence of this molecular conformation and to identify the mesophases, the molecular area, A_M, as well as

the area per mesogenic units, a_m (i.e., area occupied by one terminal unit), were calculated from X-ray and volumetric data (Table 1). The molecular area is directly deduced from the molecular volume[39] and the layer periodicity, and the area per mesogenic unit was calculated considering as above that half of the mesogenic units lie on one side, and the other half lie on the other side of the dendritic core (i.e., $4a_m = A_M$) (Table 1). It was found that in the low-temperature phase, $A_M = 90-92$ Å^2, and in the high-temperature phase, $A_M = 96-100$ Å^2, leading to the corresponding area per mesogenic unit, $a_m = 22.5-23$ Å^2 and $a_m = 24-25$ Å^2, respectively. The values of a_m, for each dendrimer in both mesophases, deduced from these calculations correspond very precisely to the expected cross sections of molten alkyl chain in both the smectic B and A phases, respectively. This result supports the correct mesophase assignments (vide supra), as well as confirms the prolate conformation of the dendrimers in both smectic phases with the peripheral anisotropic units being almost perpendicular to the layer normal direction. In this case, due to geometric constraints, the mesogenic groups of the first row of the arborescence, located in the smectic sublayer, should be tilted to match the molecular area of roughly two mesogenic groups, to occupy a larger apparent surface area (Figure 6). Of course, the rigid units contained in these aromatic slabs are tilted with respect to the layer normal, but the tilt is not correlated, that is the tilt order is short-range. In other words, the relative disordered distribution of the rigid parts yields an apparent zero tilt angle, and then a uniaxial smectic sublayer. This model is consistent with the molecular conformation deduced from MD calculations and also explains the difference between the periodicity and the molecular length. The SmB-to-SmA transformation corresponds to the loss of the hexatic order consequent to the lateral disorganization of the anisotropic units of the outer slabs.

Therefore, the morphology of the smectic phases generated by such multiblock molecules is quite unique in that it possesses a two-level molecular organization, each being dependent on the other one. It consists of an internal sublayer made of tilted rigid segments with no correlation of the tilt, flanked by outer slabs inside which the mesogenic groups are arranged perpendicular to the layer (Figure 6). Molecular modelization supports this view of strongly segregated multilayer structures, with interfaces between the various molecular parts (Figure 5). Obviously, these interfaces are not so well defined due to thermal fluctuations. Nevertheless, let us point out that, due to this peculiar structural feature, such layered mesophases cannot exactly be described as purely SmA or SmB phases.

(b) The Columnar Phase. As for the other set of dendrimers, they all showed a Col$_h$ phase, consistent with the previous described system **19f**.[35] Four (**19d**) and up to six (**19e**) sharp reflections were observed in the small-angle region, with the reciprocal spacings in the ratios 1, $\sqrt{3}$, $\sqrt{4}$, $\sqrt{7}$, $\sqrt{12}$, and $\sqrt{13}$, and they were indexed in a 2D hexagonal lattice as $(hk) = (10), (11), (20), (21), (22),$ and (31), respectively (Figure 7). In the case of **19b**, despite the fact that the columnar mesophase was monotropic and existed over a narrow temperature range of only a few degrees, it was still possible to obtain a meaningful X-ray pattern on cooling from the isotropic liquid, allowing also

(39) The molecular volumes, V_{mol}, were estimated considering a density of 1 for the molecules in the mesophase, and then were corrected by a temperature factor because the volume increases with temperature (see Table 1).
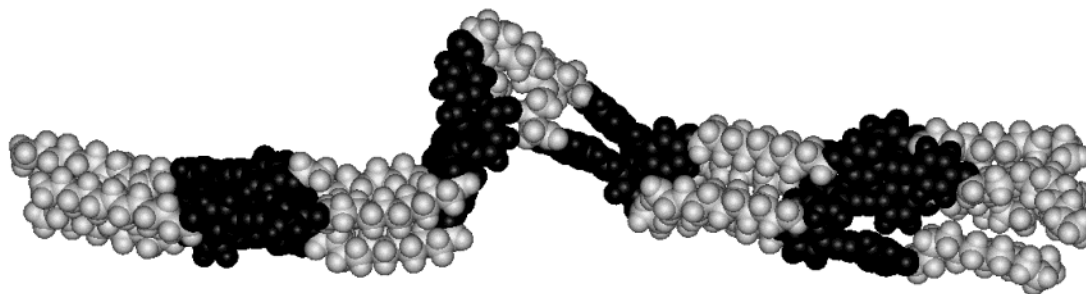
Figure 5. Snapshot of the molecular conformation of **19c** in the smectic phases obtained by molecular dynamics simulation. The parts in gray and black represent the aliphatic and aromatic parts, respectively.
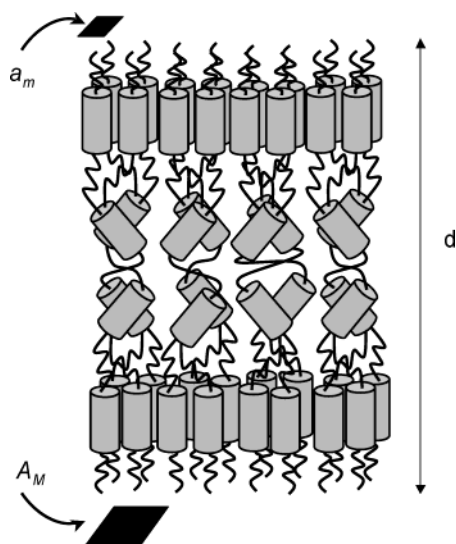

Figure 6. Model for the octopus conformation and organization within the "supersmectic" phases.
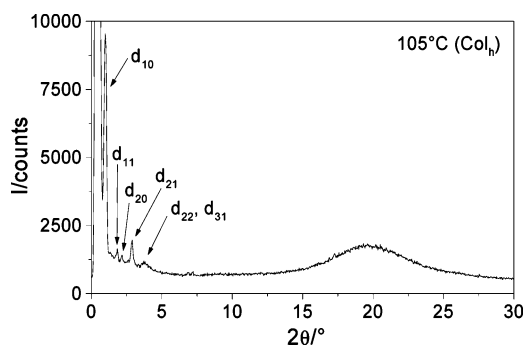

Figure 7. X-ray pattern of **19e** at 105 °C (Col$_h$).

the assignment of the phase as Col$_h$. Note that, apart from the fundamental reflection (10), the second most intense one is always the (21) reflex and is probably connected to the structure factor and must be the signature of a particular type of molecular arrangement within the columns (vide infra).[40] Similarly, the mesomorphic dendron **17e** displayed the same kind of X-ray pattern, and the same Col$_h$ phase was assigned. The results of these investigations are summarized in Table 1.

The formation of columnar mesophases in nondiscotic systems, and particularly with polycatenar mesogens,[41] is a

consequence of the mismatch between the surface areas of the aromatic cores and the cross section of the aliphatic chains, resulting in the curvature of all of the interfaces. In the present case, to compensate the discrepancy between the cross sections of both the anisometric segments and the chains, one can also imagine the former to be tilted and distributed in a "splay" fashion, with respect to the columnar axis, also resulting in the curvature of the interfaces.[42] Indeed, the parameters of the hexagonal lattices obtained experimentally, $a = 90-100$ Å, correspond fairly well to the diameter of the dendrimers in a flattened conformation, ranging between 100 and 110 Å as estimated by MD simulation (vide infra). It is therefore highly probable that the octopus preferably adopts an oblate shape within the columns that is a flattened or a wedge-like conformation with the anisotropic blocks lying more or less in the 2D hexagonal lattice plane, rather than a prolate conformation (cylindrical) as in the smectic systems. The small discrepancy between the estimated molecular diameters (100−110 Å) and the measured lattice parameters (90−100 Å) of the Col$_h$ mesophases, corresponding to a molecular contraction of about 10−20%, was ascribed to thermal fluctuations (the system is fluid and heated), that is, to the liquidlike order of the molten aliphatic chains, and to some degree of tilt of the rigid segments with respect to the columnar axis (in and out-off plane tilts) and within the lattice plane (in-plane splay or bent orientations), that is, no preferential direction and no correlation of the molecular tilt.

To propose a coherent explanation for the self-assembling of these compounds within the columns, the number of octopus able to fill a columnar slice 4.5 Å thick (*h*) was first calculated. This distance *h* is considered realistic and corresponds to the average liquidlike correlations between the peripheral mesogenic groups in liquid-crystalline phases.[18b] Let us remark that, in nondiscoid systems, a columnar slice does not have a particular significant meaning, and it does not necessarily imply that, in the present case, the columns result simply from the stacking of flat dendrimeric or supramolecular dendritic discs on top of each other, as in purely discotic materials. However, this approach permits the calculation of a linear density of occupation along the columnar axis. The molecular volumes, V_{mol}, were calculated as previously described (vide supra). The volume of one columnar stratum with a thickness (*h*) of 4.5 Å can be calculated from $S \cdot h$, where S is the columnar cross section (Table 1). The number of molecules per slice can thus be directly

(40) This peculiarity is likely connected to the onion structure of the columns, and experiments to prove this hypothesis are underway.
(41) (a) Malthête, J.; Nguyen, H. T.; Destrade, C. *Liq. Cryst.* **1993**, *13*, 171−187. (b) Nguyen, H. T.; Destrade, C.; Malthête, J. *Adv. Mater.* **1997**, *9*, 375−388.

(42) (a) Fazio, D.; Mongin, C.; Donnio, B.; Galerne, Y.; Guillon, D.; Bruce, D. W. *J. Mater. Chem.* **2001**, *11*, 2852−2863. (b) Smirnova, A. I.; Fazio, D.; Iglesias, E. F.; Hall, C. G.; Guillon, D.; Donnio, B.; Bruce, D. W. *Mol. Cryst. Liq. Cryst.* **2003**, *396*, 227−240.
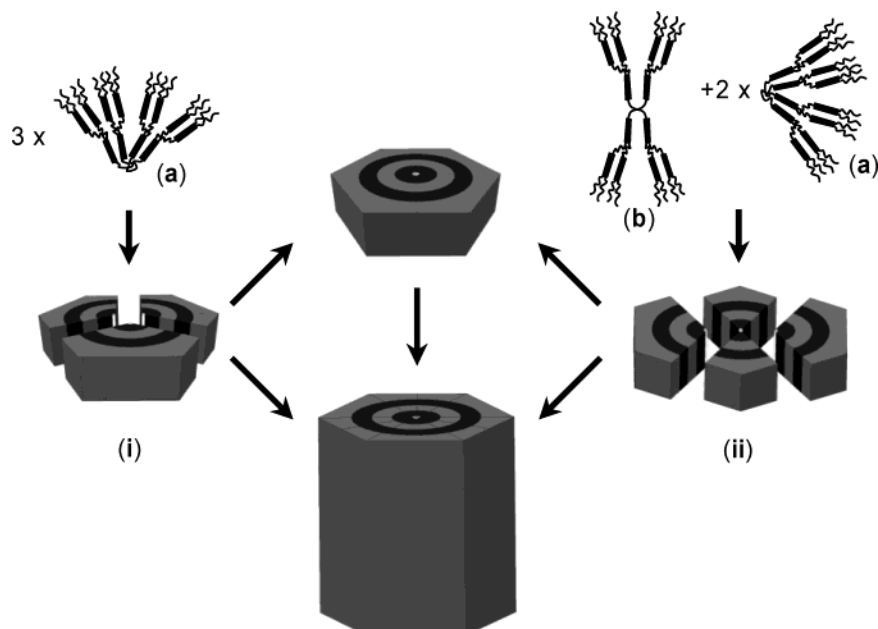
Figure 8. Schematic representation of the two possible molecular conformations of the dendrimers, (a) and (b), and their self-assembling and self-organization processes into the columns of the Col$_h$ phase, (i) and (ii).

obtained by $N = h \cdot S / V_{mol}$. It showed that, whatever the system considered, three dendrimers are necessary to fill such a columnar stratum (and six acid dendrons for **17e** as it could have been expected from our previous work[35]). Thus, because more than one molecule is needed to satisfy the dimensions of a column, the formation of the mesophase results from the self-assembling process of octopus molecules necessarily adopting predefined shapes. As the supramolecular dendrimers described by Percec et al.,[27] columnar structures are generated from the self-assembling of the most stable molecular conformations having either a wedge-like or a half-disc shape. The overall molecular conformations of the dendrimers in the mesophase are driven by the steric congestion of the terminal aliphatic chains and depend on the segregation between the different constitutive blocks. In the present case, two molecular conformations likely predominate to satisfy the geometrical requirements, the wedge-like (a in Figure 8) and the flattened (b in Figure 8) conformations. Therefore, the formation of supramolecular discs and columns results from the molecular association of these two types of dendritic conformations, as shown in Figure 8. One possibility consists of assembling three dendrimers with solely the wedge-like conformation (i in Figure 8) and another one of associating three octopus with both wedge-like and flattened conformations in a 2:1 mixture (ii in Figure 8). Clearly, one has to bear in mind that these various arrangements must coexist in the columns because it is not possible to privilege one over the other. The resultant columns then further self-organize into a 2D hexagonal lattice. Considering the diblock, alternated chemical nature of these octopus dendrimers, an onion morphology for the columns is most likely probable.

This proposed model was further justified by MD simulation: a periodic molecular model for **19d** was built from the experimental X-ray data, that is, a hexagonal lattice with a 97 Å parameter and a thickness of 4.5 Å, paved with three molecules in a flattened wedge conformation. The result of the calculation (Figure 9) evidenced a good filling of the available volume, acknowledged by a calculated density of 0.95. An

enhancement of the micro segregation over the entire simulation experiment time was also observed, contributing to the stabilization of the onion structure. Furthermore, the compensation of the molecular areas at the various interfaces at every level of the arborescence, which implies the tilt of the internal and external rigid segments with respect to the radial directions, was also shown in the modelization (Figure 9).

The case of the acid dendron **17e** is a bit puzzling. Indeed, the volume of one octopus is exactly 4 times larger than that of the precursory dendritic branch, whereas the corresponding cell volumes are in a 2-to-1 ratio (see Table 1), instead of the expected 4-to-1 ratio; a simple correlation rule clearly does not apply here. This corresponds to an important contraction (ca. 25%) of the cell parameter of the Col$_h$ formed by the octopus and that formed by the dendron. This diminution of the cell dimension may be due to the reduction of the molecular rigidity passing from the dendromesogen to the dendrimer; the rigidity of the precursory dendron would be due to cohesive and cooperative H-bondings that are due to the presence of free acid functions. Similar observations were made on an increase in the generation number (and thus the molecular volume) of the supramolecular dendrimers studied by Percec at al.[27] They did not observe a linear rule either, but on the contrary they noticed the reduction of the number of monodendrons per cell. Assuming that the molecular conformation of such dendromesogens forming the columnar structure is described as flat tapered, they explained this phenomenon by a decrease of the cone angle, and therefore by the decrease of the curvature, with increasing generation. This decrease of the curvature implicates an increase of the disc diameter (and thus of the columnar cross section), and thus more molecules to fill the disc. Here, the rigidifying of the dendron likely reduced the degree of conformational freedom, forcing them to assemble very close together (increase of the cone angle, θ_d), resulting in the reduction of the hexagonal cell, as well as an augmentation of the interfacial curvature: the tendency to pack in larger cells is then reduced (Figure 10). Once attached to the tetravalent core, each of the four branches
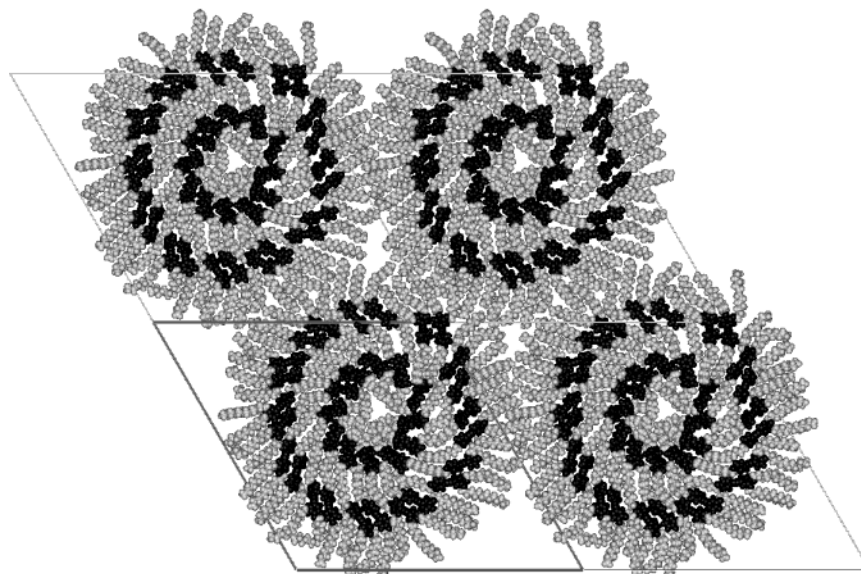
Figure 9. Snapshot of the molecular conformation in the Col$_h$ mesophase for **19d** obtained by a MD calculation. The parts in gray and black represent the aliphatic and aromatic parts, respectively.
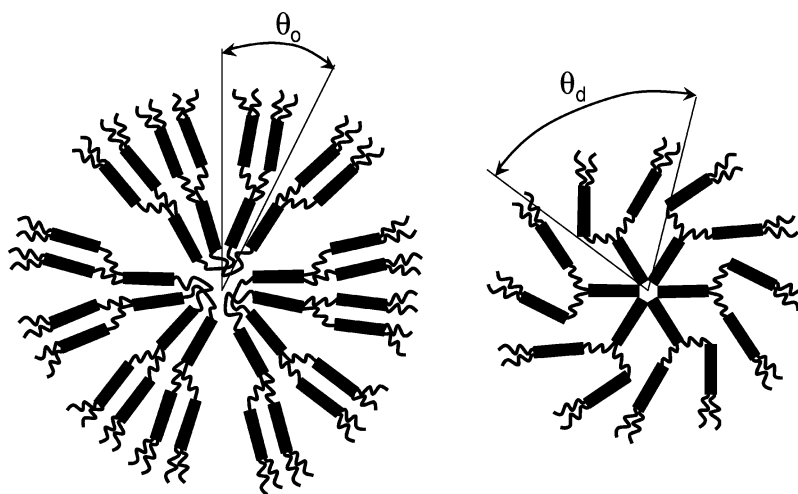

Figure 10. Effect of the cone angle on the curvature and columnar diameter.

of the dendrimers is more confined than the free branch (reduction of the cone angle, θ_o, decrease of the curvature, Figure 10), and thus a higher number of these individual branches is needed to be in accordance with the consequent larger perimeter of the columnar cross section.

Molecular Structure and Mesophase Morphology. All of the new compounds synthesized, with the exception of most of the acid precursors (except **17e**), are mesomorphic, showing either smectic-like phases or self-assembling into a columnar mesophase with a hexagonal 2D symmetry. An important result is therefore the induction of the mesomorphism upon "dendrimerization", an interesting illustration of the so-called "dendritic effect" because none of the low-molar weight monomeric components nor most of the acid precursors were mesomorphic. This result is consistent with our previous report on homolithic dendrimers.[35]

The morphology of the mesophase is determined by the number of alkyl chains grafted on the peripheral mesogenic group. Indeed, the change in the number of terminal chains per end group (one or two) modifies the relationships between the hard parts and the soft parts, and consequently the molecules will adopt either a parallel (prolate) or a flat (oblate) conformation. The formation of the smectic lamellar phases is the result of the parallel disposition of the mesogenic groups on both sides of the focal tetravalent core, the dendrimer adopting the shape of a giant elongated multipode, and then organizing into layers. In contrast, the grafting of additional terminal chains at the periphery prevents such a parallel disposition of the pro-mesogenic groups, which are forced to be radially arranged around the central moiety: the dendrimers can adopt the shape of a flat-tapered objects which will self-arrange into supramolecular discs. Although the expected mesomorphism crossover from lamellar to columnar structures was observed with an increase in the number of terminal chains,[18] the two-phase behavior or the induction of intermediate mesophases (such as the bicontinuous cubic or rectangular columnar phase,[43] for instance) is nevertheless absent within a single dendrimer.

Molecular Structure and Mesophase Stability. The stability of these mesophases results in a large part from the formation of layer-block structures being driven by microphase separation

(43) Rueff, J. M.; Barberá, J.; Donnio, B.; Guillon, D.; Marcos, M.; Serrano, J. L. *Macromolecules* **2003**, *36*, 8368−8375.
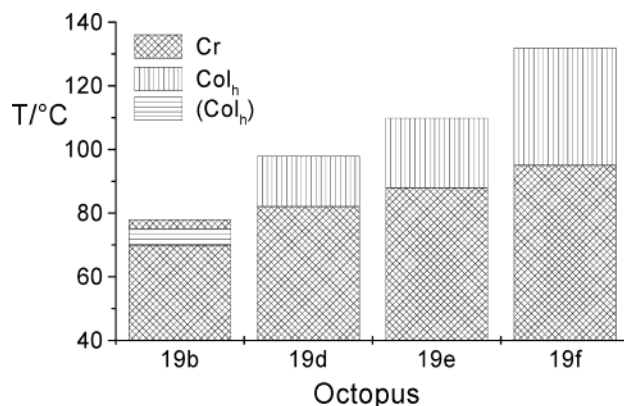
Figure 11. Evolution of the mesophase stability from tolane-rich (**19b**, **19d**) to stilbene-rich (**19e**, **19f**) octopus LCDs. The brackets indicate that the mesophase is metastable (monotropic).

between the noncompatible constituting segments of the molecule, which is at each hierarchical level reinforced by the specific anisotropic interactions between the rigid mesogenic units. An octopus with one chain per end group has been found to be more stable than those with two chains per end group probably due to an optimization of the lateral interactions for the former.

Another interesting observation is the continuous increase of the thermodynamic stability of the mesomorphism in relation to the increasing number of stilbene units in the dendrimer at the expense of tolane groups. Indeed, whatever the system being considered, neither the type of the building blocks (tolane or stilbene) nor their spatial disposition (alternated in the multicomponent heterolithic systems) affects the nature of the mesophase, but does modify substantially the mesophase stability. In the case of the smectic systems, generalization is not made possible because only two molecules (vide supra) were synthesized, although this tendency is nevertheless perceptive. However, in the case of the columnar systems, the impact of the octopus topology on the mesophase stability is obvious (Figure 11). Indeed, **19b**, containing 100% of tolane units, exhibits a monotropic Col_h phase, whereas, for **19d** (66.6% tolane-rich), **19e** (33.3% tolane-rich), and **19f** (100% stilbene-rich), both transition temperatures increase, the clearing temperature increasing at a faster rate than the melting temperature, resulting in a net enhancement of the mesomorphic temperature range. This is likely a consequence of the greater flexibility of the stilbene units, favoring more efficient and less constrained intermesogen interactions than the tolane species, which is too rigid. It is therefore possible to tune and control the mesomorphic properties of these octopus dendrimers by a subtle modular construction.

Conclusions

Several novel liquid-crystalline octopus dendrimers, with both homolithic and heterolithic structures, have been synthesized, containing stilbene and/or tolane groups as basic elementary subunits. They were obtained by a modular construction, consisting of the preparation of the acid branches and their subsequent grafting onto a tetravalent core through amido linkages. They showed smectic or columnar phases with unusual morphologies (smectic with a two-level ordering and onion-like columnar phases) depending on the substitution pattern of the terminal groups. The transition temperatures and mesophase

stability were found to be influenced by the nature and the relative disposition of the anisotropic segments within the dendritic matrix.

As previously demonstrated, the high density of aliphatic chains likely imposes curved interfaces at all hierarchical levels of the dendrimers, that is, between the pro-mesogenic units, the aliphatic spacers, and the terminal chains, respectively, forcing the molecules to adopt a wedge-like conformation, and thus promoting their self-assembling toward a columnar organization with an onion internal morphology. As for the smectic-like phases, the dendrimers adopt a parallel conformation, and, due to the particular nature of the molecules, the segments of the first generation, which are located in the smectic sublayer, are tilted, leading to a two-level molecular organization.

This structural concept proves to be innovative and versatile as it offers many new opportunities in the design of a wide range of multicomponent systems with specific properties for potential novel applications. Indeed, it appears that large flexibility and freedom are allowed in the choice of the elementary anisotropic bricks forming the dendritic skeletons of these LCDs, without the suppression of the mesomorphic properties. Additionally, such bricks can be independently interchanged, and the stability of the mesophases accordingly modulated, probing the good sensitivity of the dendritic scaffold with the nature and the mutual arrangement of the mesogenic segments (spatial location), and the intimate relationships with the mesomorphic properties. The high sensitivity of such AB-block co-dendrimers to the surrounding environment (properties versus molecular structure) could be, in principle, beneficial to access to some kinds of molecular sensors, that is, to use such supermolecules as tools to test how properties in general may be altered or modulated upon delicate external stimuli.

Future studies should examine the synergic and/or cooperative effects upon the insertion of various types of functional bricks. The effects of the branching cell multiplicity as well as the nature of the core (connectivity, structure) are currently under investigation and will be reported in due course. We have now showed that the concept works for homolithic as well as for alternated heterolithic systems. It is now envisaged to prepare segmented "block-type" co-dendrimers, where each of the two dendritic branches (of same or different generation) contains different mesogenic units in different locations, with different terminal chain substitution patterns and topologies of attachment to the core. However, an important effort should be made toward the selective chemistry of the core to access to such systems.

Experimental Section and Method of Characterization

The synthesis of the elementary bricks, monodendrons, and final dendrimers, their structural analysis, and the various techniques used for their analytical characterization and for the structural determination of the mesophases structures have been deposited as Supporting Information.

Supporting Information Available: Experimental section containing techniques, materials, the synthesis and analytical characterization for all organic precursors, monodendrons, and dendrimers, and optical textures (PDF). This material is available free of charge via the Internet at http://pubs.acs.org.